Formation of self-assembled epitaxial nickel nanostructures

H. Zhou,[a] D. Kumar, A. Kvit, A. Tiwari, and J. Narayan
Department of Materials Science & Engineering, North Carolina State University, Raleigh, North Carolina 27695-7916

(Received 11 April 2003; accepted 23 July 2003)

Highly orientated nickel magnetic nanoparticles were obtained by pulsed laser deposition technique on silicon (100) substrate using epitaxial titanium nitride film as the template. These nanoparticles have been characterized by conventional and high-resolution transmission electron microscopy, scanning transmission electron microscopy Z-contrast imaging, and x-ray diffraction techniques. The results have shown that the growth of nickel on epitaxially grown titanium nitride follows a three-dimensional island growth mechanism. The predominant orientation of nickel islands observed is Ni(100)‖TiN(100)‖Si(100), the so-called ''cube-on-cube'' orientation relation. The islands are faceted with a truncated pyramidal shape and bounded by (111) planes at sides and (100) plane at the top. Islands with nontruncated pyramidal shape were also found in some samples, but with rotational orientation relations, where the nickel crystal rotates with an approximate angle of 90° with respect to one of TiN ⟨110⟩ directions parallel to the interface. The appearance of this rotational epitaxial growth did not show any obvious deposition temperature dependence in the range of 400–650 °C, rather it seemed to be closely related to the crystalline quality of TiN template. The actual size of islands varies from a few nanometers to tens of nanometers, depending on the deposition time and temperature. The three-dimensional growth of nickel islands and the island faceting could be explained by the surface energy anisotropy of both nickel and titanium nitride. © *2003 American Institute of Physics.* [DOI: 10.1063/1.1609046]

I. INTRODUCTION

It is well known that for heteroepitaxial growth, there are three basic modes: (1) two-dimensional layer-by-layer growth ($F-M$); (2) three-dimensional island growth ($V-W$); and (3) two-dimensional (2D) followed by three-dimensional (3D) growth (layer-by-layer plus islands) ($S-K$). The film growth mode depends on the surface free energy of the substrate and the film, as well as the interfacial energy. There have been intense interests in the latter two growth modes during last decades due to their ''self-assembly'' nature, which provides possible routes to fabricate oriented nanostructures without needing masking and patterning. $S-K$ growth is of special interest because the dislocation-free islands can be formed during early stages of growth. However, the condition for $S-K$ growth is very demanding since it is the misfit strain accumulated in the system that finally induces the transition in the growth mode from 2D to 3D (the strain here is relieved first by forming islands rather than dislocations).[1–5] So far, most of the work on self-assembly has been conducted on a few semiconductor systems, such as Ge/Si, InAs/GaAs, InGaAs/GaAs, which were found to grow by $S-K$ mode. The focus of these studies were their growth mechanism, optical properties, and electronic structures.[5–16] For $V-W$ growth, there are fewer constraints. Since the large misfit between the substrate and the film could be accommodated by interface dislocations,[17,18] the surface energy of the system plays an important role in determining whether the system is favoring 3D growth. Therefore, the self-assembled 3D epitaxial growth is a promising way for producing nanostructures, where size and distributions can be controlled in a systematic way, especially in the applications where defect (dislocation)-free interface is not that critical for the device performance.

Nanomagnetic materials have drawn significant attention in recent years due to the expectation of their possible applications in ultrahigh density information storage. The development of effective and reproducible methods of fabrication of magnetic nanostructures with controlled properties is highly desirable. In our previous studies,[19,20] magnetic measurements and analyses were conducted on the samples containing nickel nanoparticles embedded in epitaxially grown titanium nitride matrix. The results were compared with that of the nickel particles of similar size embedded in amorphous alumina matrix. It was found that the sample containing particles grown in epitaxial titanium nitride matrix had a considerably higher blocking temperature and coercivity, which was considered to be largely attributed to the highly oriented nature of nickel particles. In this paper, we focus on the growth aspects of the nickel particles grown on epitaxial titanium nitride templates, with emphasis on growth modes, orientations and crystal equilibrium shapes. The goal of our investigation is the development of a method to produce self-assembled 3D orientated metal nanostructures in a controlled way for a variety of applications ranging from nanomagnetics to spintronics.

[a]Author to whom correspondence should be addressed; electronic mail: hzhou4@unity.ncsu.edu

II. EXPERIMENTS

Titanium nitride and nickel were deposited sequentially on silicon (100) substrates in a pulsed laser deposition (PLD) system using a multitarget facility. The substrates preparation procedure includes ultrasonically degreasing and cleaning in acetone and methanol followed by a short time etching in a hydrofluoric acid solution (49% HF) to remove the surface silicon dioxide layer. The main deposition parameters are as follows: vacuum before and after substrate heating was around 5×10^{-7} and 5×10^{-6} Torr, respectively; laser beam had an energy density of $\sim 2\ \mathrm{J/cm^2}$ and a repetition frequency of 10 Hz. For studying the effect of deposition temperature on the nickel crystal growth, the deposition temperature for Ni was varied in the range of 400–650 °C. In order to minimize the effects of the template crystalline quality on the nickel crystal growth, the deposition temperature for TiN was fixed at 600 °C, which was found to be an optimized temperature for TiN epitaxial growth on Si (100).[21] The thickness of TiN template layer was in the range of 25–40 nm (corresponding to a deposition time of about 1.5–2 min). The size of Ni particles was expected to vary with the nominal thickness of nickel layer, which was adjusted again by varying the deposition time ranging from 20 to 45 s.

The morphology, size and orientation of nickel particles, as well as the crystalline quality of the template were studied by conventional transmission electron microscopy (TEM) and high-resolution TEM (HRTEM) using TOPCON 002B and JEOL 2010F. X-ray diffraction (θ–2θ scan) was used to determine the crystalline quality for a larger area of the sample although it can only provide the texturing information along the growth direction. The interface between nickel particles and the titanium nitride template was studied by scanning transmission electron microscopy (STEM) *Z*-contrast imaging and electron energy loss spectroscopy-(EELS) in the JEOL 2010F. The samples for the cross-sectional TEM study were prepared by mechanical polishing, followed by Ar ion milling to electron transparency.

III. RESULTS AND DISCUSSION

A. Nickel crystal growth mode

⟨011⟩ zone axis cross-sectional TEM study showed that while titanium nitride formed a continuous layer on the silicon substrate, nickel exhibited the island growth mode in the whole temperature range under our investigation (400–650 °C). Hereafter, we will call these nickel crystals ''islands.'' Shown in Fig. 1 are the representative ⟨011⟩ zone axis images of Ni islands grown on a continuous TiN template layer. It is clearly seen that nickel islands are faceted with a truncated pyramidal shape. Non-truncated pyramidal islands were also observed and have been reported earlier.[19,20] These nontruncated pyramidal islands were found to have different orientations from that in truncated pyramidal shaped structures as discussed later. The lateral size of islands actually varies from a few nanometers to tens of nanometers, depending on the deposition time chosen. Some apparently large size islands observed in samples deposited at lower temperatures were found to be a result of coalescence between neighboring islands. The height distribution of islands is much narrower than that of lateral size. The height/lateral size aspect ratio shows weak temperature dependence in the temperature range of our investigation: the aspect ratio is bigger for the samples deposited at higher temperatures. The separation between islands is expected to be larger than it appears in the cross-sectional TEM image due to the projection overlapping. The interface between TiN and Ni shown in the *Z*-contrast image in Fig. 1(b) is quite sharp, which means no significant interfacial reaction occurred during deposition since the intensity of *Z*-contrast image is proportional to the square of the atomic number. It is worth noting that there is no wetting layer of nickel observed in the STEM *Z*-contrast image, which is in agreement with the EELS analysis (not shown here). Therefore, we conclude that the growth of nickel on epitaxially grown titanium nitride is three-dimensional in accordance with the $V-W$ mode.

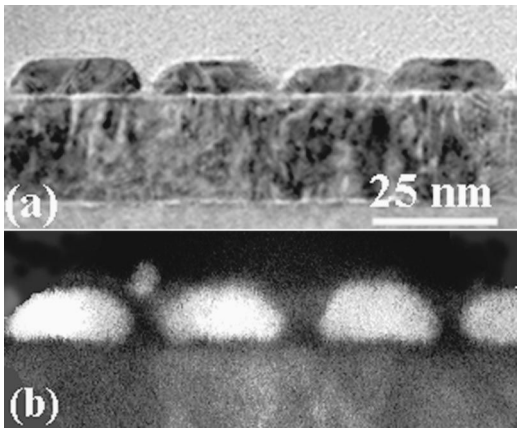

FIG. 1. Images of truncated pyramidal shaped nickel islands grown on titanium nitride template layer: (a) low-magnification TEM and (b) STEM *Z*-contrast image. Note that both of the images were taken in Si ⟨011⟩ zone axis, but not from the same area.

During epitaxial growth, whether the deposited material adopts the form of a thin continuous film or separated islands is determined by the interfacial free energy as well as the surface free energies of both substrate and film material. For an epitaxial interface, the interfacial energy is closely related to the atomic configuration in the interface region since it affects many energy terms, such as the electronic structure of interface atoms, interfacial atomic bonding strength, and the lattice strain. The interface atomic configuration is a direct result of the interface coherency, e.g., how much the lattice is distorted and how many misfit dislocations are formed in the case of a semicoherent interface. There are very few data of the interfacial energy reported partially because the experimental techniques available are limited and theoretical calculations need the exact information about the atomic configuration and the strain states, which varies for each individual system. Here we will examine the growth condition only in light of the surface energy of both the substrate and the film, assuming that interfacial energy is fixed. The data on the surface free energy as a function of orientation that we have obtained from the literature[22–24] are mostly theoretically calculated, and they depend strongly on which

TABLE I. Surface energy values obtained from the references.

Materials	Surface energies ($J\,m^{-2}$) 100	110	111	Method	Reference No.
Si	1.36	1.43	1.23	Experiments	22
	1.34	1.573	1.41	Calculations	
	1.488	1.721	1.405	Calculations	
TiN	1.06,[a] 1.53[b]	2.59,[a] 2.87[b]	4.59,[a] 5.08[b]	GGA,[c] RPBE[d]	23
	1.28,[a] 1.75[b]	2.85,[a] 3.13[b]	4.92,[a] 5.42[b]	GGA,[c] PBE[d]	
	1.30,[a] 1.76[b]	2.86,[a] 3.14[b]	4.95,[a] 5.45[b]	GGA,[c] PW91[d]	
Ni	2.426	2.368	2.011	GGA,[c] FCD[e]	24

[a]For relaxed geometries.
[b]For unrelaxed geometries.
[c]Generalized gradient approximation.
[d]Refer to different functional forms used for GGA, check the corresponding reference for details.
[e]Full charge density.

theory, model and assumptions they were based on. Therefore, we can not compare the absolute values from different sources where different calculation techniques were used. However, it should give the right estimates if the comparison is done for the data from the same source. Table I lists the surface free energies for some low index facets of silicon, titanium nitride and nickel obtained from the literature.[22–24] It is easily seen that there is significant differences in the surface energy between the different facets of TiN, a phenomenon not found in silicon and nickel. Even the unrelaxed TiN (100) surface has a relatively low surface free energy, around $1.53-1.76\,J\,m^{-2}$, while that of TiN(110) and TiN(111) are several times higher [$2.87-3.14\,J\,m^{-2}$ and $5.08-5.45\,J\,m^{-2}$ for (110) and (111), respectively].[23] This could partially explain our result that TiN has a very strong tendency to epitaxially grow on Si (100) by 2D mode, while on the top of TiN (100), Ni tends not to wet the low energy stable surface by growing in 3D mode. The fact that deposited nickel takes an island growth mode could also be explained by the surface energy data of nickel itself:[24] among the different facets of nickel crystal, it is the (111) facet, rather than the (100) facet, which has the lowest surface energy. The surface energy anisotropy of nickel is also the determining factor for the island faceting, which will be discussed later in detail.

B. Nickel crystal epitaxial orientation

Figure 2 is a typical x-ray diffraction (XRD) spectrum of a deposited sample, which clearly shows that both TiN and Ni are highly textured along the growth direction (Si (100)) since there is no other diffraction peaks observed except TiN (200), TiN (400), and Ni (200). It should be mentioned that the θ–2θ scan in Fig. 2 provides information on alignment only in the direction normal to the surface. Results obtained from TEM studies, which can provide the alignment information in all three directions, are shown in Fig. 3. Figure 3 is a $\langle 011 \rangle$ zone axis high-resolution image of a nickel island with the inset showing a cross-sectional selected area electron diffraction pattern taken from areas containing silicon, titanium nitride, and nickel. The alignment of diffraction spots of Si, TiN, and Ni indicates that the predominant epitaxial orientation for both TiN and Ni is "cube-on-cube," that is all three (100) axes of film are parallel to those of silicon substrate. This cube-on-cube orientation relation can be clearly seen from the lattice fringes in the high-resolution image. Other orientations for nickel island growth have been also observed.[19,20] In these cases, the (111) planes of nickel crystallites tilted themselves about a certain angle toward the TiN/Ni interface. From the crystallographic point of view, this orientation is the result of a rotation of nickel crystallites (typically by 83° or 90°) on one of TiN $\langle 011 \rangle$ directions parallel to the interface (zone axis of cross-sectional TEM study). We will call this kind of orientation "rotational orientation" hereafter. The appearance of these rotational oriented islands seemed not to depend on the deposition temperature, at least in the range of our investigation.

Silicon has a diamond structure with a lattice constant 0.543 nm and titanium nitride has a sodium chloride structure with a lattice constant 0.424 nm and their lattice mismatch is as large as 22%. The epitaxial growth of titanium nitride on Si (100) is achieved by domain matching epitaxy mechanism, where integral multiples of major lattice planes match across the interface.[17,18,21] The misfit between nickel,

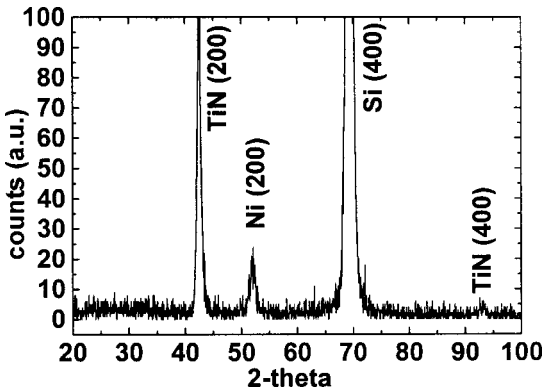

FIG. 2. X-ray diffraction data from a sample with a layer of nickel islands grown on silicon (100) substrate using epitaxial titanium nitride as template, which indicates that TiN and Ni are highly textured along the growth direction (Si (100)).

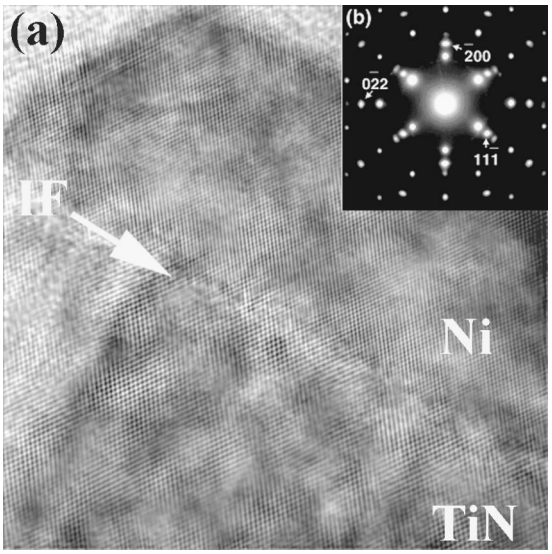

FIG. 3. Si ⟨011⟩ zone axis HRTEM image of a cube-on-cube oriented nickel island grown on the epitaxial titanium nitride template. The inset is a cross-sectional electron diffraction pattern taken from an area containing silicon substrate, titanium nitride template, and nickel islands. The alignment of diffraction spots of Si, TiN, and Ni clearly indicates the cube-on-cube epitaxial orientation relation for both TiN and Ni.

which has a simple face-centered cubic (fcc) structure with a lattice constant of 0.352 nm, and titanium nitride is 17%, far beyond the critical strain (7%–8%) of conventional one-to-one lattice mismatching. Therefore, domain matching epitaxy should also be expected for nickel island growth, which was indeed observed. Figure 4 is an amplified ⟨011⟩ zone axis HRTEM image of Ni/TiN interface, which clearly shows the misfit dislocations distributed along the interface [the small black arrows indicate the extra (111) lattice planes].

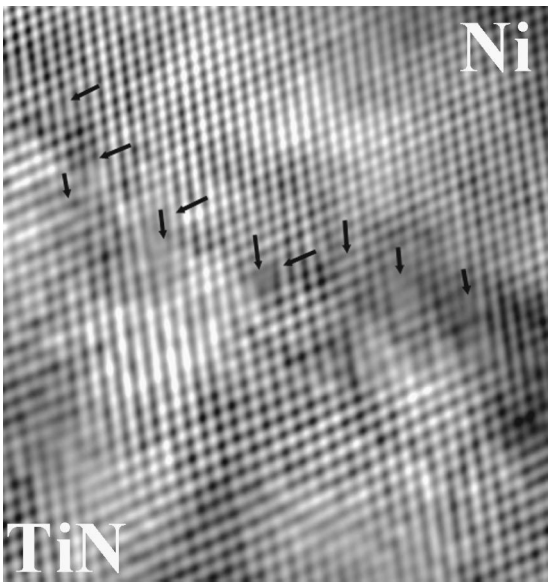

FIG. 4. Amplified ⟨011⟩ zone axis HRTEM image of an interface between a cube-on-cube oriented nickel island and the titanium nitride template. Small black arrows indicate extra (111) lattice planes. It is clearly seen that these are 60° dislocations with a Burgers vector $a/2\langle 110\rangle$ lying in (111) planes. Some of dislocations appear in pairs combining at the interface to form a 90° dislocation with Burgers vector $a/2\langle 110\rangle$ lying in (100) plane.

The domain size varies a lot, from 4TiN/5Ni, 5TiN/6Ni to 6TiN/7Ni and even 7TiN/8Ni. This big variation in domain size is possibly due to two reasons: local topographical features in the TiN surface (such as steps), and the special nature of 3D island growth, in which the dislocations may be generated at the edge of islands.[25] The first reason is more likely true since in HRTEM images of the interface, steps are indeed seen accompanied by a significant change of domain size. The Burgers vector of those dislocations is $a/2\langle 110\rangle$ lying in (111) planes (60° dislocation). These dislocations usually appear in pairs (in two sets of (111) plane) and combine at the interface to form a 90° dislocation with Burgers vector $a/2\langle 110\rangle$ lying in (100) plane.

In the case of heteroepitaxial thin film growth, there are several factors that will affect the epitaxial orientation, such as lattice misfit, interfacial atomic bonding, and even the atomic mobility, which is determined by both the thermal energy of the atoms and the substrate surface local roughness (topographical features of the substrate). In all cases where nickel grows via rotational orientation, two sets of (111) planes have tilted themselves to a smaller inclination angle with respect to the template surface compared to that of the cube-on-cube case, and as a result the lattice misfit has been considerably reduced. However, the predominant orientation of nickel epitaxial growth is still cube-on-cube. Therefore, the lattice misfit could not be the determining factor here. It was observed that the interface between a rotational grown nickel island and its underneath titanium nitride is relatively rougher than that for "cube-on-cube" oriented islands. Besides, the rotational epitaxial growth tends to occur in the samples where silicon substrate cleaning was not good, or in the multilayer samples where epitaxy deteriorated with increasing number of grown layers. These facts suggest that the local structure in the template surface plays an important role. The local atomic structure of the template surface could directly affect the interfacial inter-atomic bonding length, and therefore bonding energy.[26] The topographical features could also influence the nucleation site and the mobility of the adatoms. Further investigation of the interface and interface modeling is necessary to obtain a detailed mechanism.

C. Nickel island faceting

It was also found that the morphology of an island is closely related to its orientation. The truncated pyramidal shaped islands are cube-on-cube oriented, while those non-truncated shaped were grown via rotational orientation.[19,20] It is clearly seen from HRTEM images that the cube-on-cube oriented (truncated pyramidal) islands are bounded by (111) planes at sides and (100) plane at the top. In the case of rotational orientated islands, the bounding lattice planes of the pyramidal shaped islands are also (111) facets. The difference lies in the angles formed by the two facing (111) planes: the angle for cube-on-cube oriented (truncated pyramidal) islands is 70.52° and that for rotational orientated (pyramidal) islands is 109.48°, which is schematically shown in Figs. 5(a)–5(c). This was also supported by the result of angle measurements from the TEM low-magnification images, where the inclination angle of the side

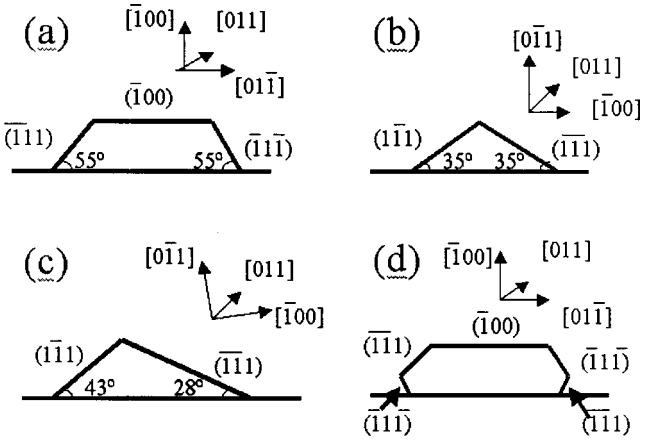

FIG. 5. Schematic of nickel faceting: (a) a truncated pyramidal shaped island with the cube-on-cube orientation; (b) a pyramidal shaped island with rotational orientation (90° rotation); (c) a pyramidal shaped island with rotational orientation (83° rotation), and (d) small (111) facets near the edges, the areas are exaggerated.

wall for truncated pyramidal islands is around 55°, which is close to the calculated theoretical value 54.74°. Since the deposition was carried out at elevated temperatures (400–650 °C) and there is no capping layer on the top of the nickel islands, it is reasonable to consider these islands having equilibrium shapes, the shape that minimizes the total surface energy at a fixed volume. If the kinetic factors that impede the atoms from moving around freely are negligible, this shape should be determined by the surface energy anisotropy of nickel crystal. Here the adsorbate impurity induced faceting effect could be neglected. Under the deposition vacuum (10^{-6} Torr), the gaseous impurities impingement rate is approximately 10^{14} molecules/cm^2 s,[27] compared to the estimated peak deposition flux of 10^{19} atoms/cm^2 s. The surface energy data of Ni listed in Table I is from Vitos and co-workers' work,[24] calculated by full charge density in generalized gradient approximation method. Their results showed that for nickel, (111) facets have the lowest surface energy compared to (100) and (110) facets. Therefore, it is understandable that these islands tend to grow in the way that (111) planes formed a large percentage of surface (serving as side walls). Unlike the cube-on-cube oriented islands, the islands grown by rotational orientation do not have a flat top. From the crystallographic point of view, after a close to 90° rotation, the growth direction of these islands is not the ⟨100⟩ direction anymore. As a result, if there is a "flat top," it should be the (110) surface rather than the (100) surface, as shown in Figs. 5(b) and 5(c). Therefore, we deduce that Ni (110) surface should have higher surface energy than Ni (100) although the theoretical calculations made by Vitos *et al.*[24] shows the opposite [2.368 J cm^{-2} for Ni (110) and 2.426 J cm^{-2} for Ni (100)].

There is another interesting observation. In many cases, we have observed "recesses" in the bottom edges of the islands, as schematically shown in Fig. 5(d). From HRTEM images and the angle measurement in low magnification images, it is easily seen that these planes are also (111) planes. This could be explained again by energetics considerations. After forming these recesses, the energy of the whole system is reduced as a result of replacing some of the high energy interface area by TiN (100) and Ni (111) surface, which are energetically more stable.

IV. CONCLUSION

In summary, we have produced highly orientated nickel magnetic nanocrystallites by nickel epitaxial growth on Si (100) using an epitaxially grown TiN as the template layer. The growth of nickel was found to be in accordance with $V-W$ three-dimensional island growth mode since no wetting layer was observed in STEM Z-contrast images and EELS analysis. The predominant epitaxial orientation determined by both electron diffraction and XRD is cube-on-cube with Ni(001)‖TiN(001)‖Si(001). Other rotational orientations, where the nickel crystallites rotate with an approximate angle of 90° with respect to one of TiN ⟨011⟩ directions parallel to the interface, were also observed in some samples. The appearance of this rotational epitaxial growth did not show any dependence on the deposition temperatures in the range of our investigation, rather it seemed to be closely related to the crystalline quality of TiN template. We suggest that the local structure of the template, in terms of atomic configuration and topographical feature, is responsible for this rotational orientation. The morphology of an island is orientation dependent. The truncated pyramidal shaped islands are cube-on-cube oriented, while those non-truncated shaped were grown via rotational orientation. The HRTEM study and angle measurements from the low-magnification images showed that the nickel islands are bounded by (111) planes, and terminated by (100) plane at the top in the case of truncated pyramidal shaped islands. The three-dimensional growth of nickel islands and the island faceting could be explained by the surface energy anisotropy of both nickel and titanium nitride. Depending on the deposition time and temperature chosen, the size of islands can vary from a few nanometers to tens of nanometers with a quite narrow size distribution. From the results of our study, we conclude that three-dimensional epitaxial growth of metal is a promising way to produce highly orientated magnetic nanostructures with uniform sizes and separations.

[1] S. Christiansen, M. Albrecht, H. P. Strunk, P. O. Hansson, and E. Bauser, Appl. Phys. Lett. **66**, 574 (1995).
[2] L. J. Gray, M. F. Chrisholm, and T. Kaplan, Appl. Phys. Lett. **66**, 1924 (1995).
[3] S. Luryi and E. Suhir, Appl. Phys. Lett. **49**, 140 (1986).
[4] J. Tersoff and F. K. LeGoues, Phys. Rev. Lett. **72**, 3570 (1994).
[5] D. J. Eaglesham and M. Cerullo, Phys. Rev. Lett. **64**, 1943 (1990).
[6] Y.-W. Mo, D. E. Savage, B. S. Swartzentruber, and M. G. Lagally, Phys. Rev. Lett. **65**, 1020 (1990).
[7] D. J. Eaglesham, F. C. Unterwald, and D. C. Jacobson, Phys. Rev. Lett. **70**, 966 (1993).
[8] M. Goryll, L. Vescan, K. Schmidt, S. Mesters, H. Lüth, and K. Szot, Appl. Phys. Lett. **71**, 410 (1997).
[9] V. Le Thanh, P. Boucaud, D. Débarre, Y. Zheng, D. Bouchier, and J.-M. Lourtioz, Phys. Rev. B **58**, 13115 (1998).
[10] A. Madhukar, Q. Xie, P. Chen, and A. Konkar, Appl. Phys. Lett. **64**, 2727 (1994).
[11] D. Leonard, K. Pond, and P. M. Petroff, Phys. Rev. B **50**, 11687 (1994).
[12] D. Leonard, M. Krishnamurthy, S. Fafard, J. L. Merz, and P. M. Petroff, J. Vac. Sci. Technol. B **12**, 1063 (1994).
[13] D. Leonard, M. Krishnamurthy, C. M. Reaves, S. P. Denbaars, and P. M. Petroff, Appl. Phys. Lett. **63**, 3203 (1993).

[14] P. Hawrylak and A. Wojs, Semicond. Sci. Technol. **11**, 1516 (1996).
[15] B. V. Volovik *et al.*, Semicond. Sci. Technol. **16**, 186 (2001).
[16] A. E. Zhukov *et al.*, Semicond. Sci. Technol. **14**, 575 (1999).
[17] J. Narayan and S. Oktyabrsky, J. Appl. Phys. **92**, 7122 (2002).
[18] J. Narayan and B. C. Larson, J. Appl. Phys. **93**, 278 (2003).
[19] D. Kumar, H. Zhou, T. K. Nath, A. Kvit, and J. Narayan, Appl. Phys. Lett. **79**, 2817 (2001).
[20] D. Kumar, H. Zhou, T. K. Nath, A. Kvit, and J. Narayan, J. Mater. Res. **17**, 738 (2002).
[21] J. Narayan, US Patent No. 5,406,123 (11 April, 1995).
[22] D. J. Eaglesham, A. E. White, L. C. Feldman, N. Moriya, and D. C. Jacobson, Phys. Rev. Lett. **70**, 1643 (1993).
[23] M. Marlo and V. Milman, Phys. Rev. B **62**, 2899 (2000).
[24] L. Vitos, A. V. Ruban, H. L. Skriver, and J. Kollár, Surf. Sci. **411**, 186 (1998).
[25] F. K. LeGoues, M. C. Reuter, J. Tersoff, M. Hammar, and R. M. Tromp, Phys. Rev. Lett. **73**, 300 (1994).
[26] T. Zheleva, K. Jagannadham, and J. Narayan, J. Appl. Phys. **75**, 860 (1994).
[27] Gaseous impurities impingement flux $\Phi = 3.513 \times 10^{22} P/\sqrt{MT}$ molecules/cm^2 s, where P is the vacuum expressed in torr, M is the molecule weight of the gaseous impurity, and T is the temperature expressed in K.